Wood Science and Technology (2023) 57:1299–1317
https://doi.org/10.1007/s00226-023-01488-0

ORIGINAL

Evaluating the quality of surface carbonized woods modified with a contact charring or a gas flame charring technique

Maija Kymäläinen[1] · Jakub Dömény[2] · Matthew Schwarzkopf[3] · Vit Šeda[2] · Lauri Rautkari[1]

Received: 14 October 2022 / Accepted: 8 August 2023 / Published online: 15 September 2023

Abstract

Surface carbonization, or charring, of wooden exterior cladding boards is a modification method that creates a fully organic barrier layer in resemblance to a coating. The process effectively degrades the wood and transforms it into a carbonaceous residue that protects the underlying unmodified wood from environmental stresses. The surface quality of wood modified in this manner is a combination of several factors and depends on the manufacturing method and wood species. To assess the quality of spruce and birch modified with contact and flame charring techniques, several experiments were set up from the nanoscale to macroscopic evaluation of surface resistance to different stresses. The changes in elemental composition are scaled with the modification severity with little differences between wood species. The carbon structures analyzed by high-resolution transmission electron microscopy (HR-TEM) were found to be amorphous, but the electron energy-loss spectroscopy (EELS) revealed higher ordering with what is assumed to be random graphitic stacking of carbon sheets. These carbon–carbon bonds are stable, so a higher ordering is hypothesized to induce improved resistance to exterior stresses. The scanning electron microscopy (SEM) revealed a clear difference between contact-charred and flame-charred woods. The selected contact charring temperature was not high enough to induce the transformation of cell walls from anisotropic into an isotropic material but provided other benefits such as a relatively crack-free, smooth and scratch resistant surface. Surface roughness was able to adequately predict the surface quality of the contact-charred samples, and scratch tests were found to be suitable for evaluating the mechanical stress resistance of the surface instead of abrasion. In terms of overall quality, birch instead of spruce was concluded to better respond to both charring methods, although contact charring eliminates some species-specific characteristics, resulting in more homogeneous surfaces.

Extended author information available on the last page of the article

Introduction

One-sided surface charring of wood has been raising interest as a natural, esthetic and functional modification method for exterior cladding boards. In the process, a carbonaceous residue is formed which protects the underlying wood from adverse effects of weather and moisture. This char layer acts as a barrier layer in resemblance to an applied coating. In practice, there are two methods for carbonizing the wood surface: a flame and a contact charring technique. The flame charring technique may resemble the traditional Japanese charring method of *yaki sugi* with triangular board towers and ignition fires (Ebner et al. 2021, 2022), or a more efficient method using gas-fired torches (Kampe and Pfriem 2018; Kymäläinen et al. 2022a). The downside of this "open-flame" method is the relative unpredictability of the result, as wood species- and structure-dependent factors may lead to a heterogeneous surface. If the treatment is applied too quickly, it leaves denser parts such as knots insufficiently charred, whereas if applied too slowly, it reduces the thickness of the wood as the carbon on the surface is consumed and ash is formed. To address these issues, a contact charring technique has been proposed (Kymäläinen et al. 2017, 2018, 2020, Čermak et al. 2019, Machová et al. 2021; Šeda et al. 2021; Kymäläinen et al. 2022a). The process utilizes a heated surface that can consistently maintain a targeted temperature for the desired treatment duration. The resulting surface is hard, smooth and hydrophobic due to flow and plasticization of structural components and migration and condensation of extractives (Kymäläinen et al. 2018, 2022c). This method is still under development, but the experimental pilot scale results presented by Kymäläinen et al. (2020) were promising for potential commercial development. One challenge of further experimental development is the lack of a satisfactory metric for quantifying the effect of these modifications in terms of quality.

Wood surface quality is an important indicator of service life for wood used as claddings, as it largely dictates the performance in use in terms of mechanical and biological durability as well as esthetic aspects. The term "quality" is used with different connotations depending on the specific study field, but considering wood products, it usually stands for surface roughness/smoothness that affects further processing such as milling, bonding or adhesion (Hiziroglu et al. 2013; Salca and Hiziroglu 2014; Kvietková et al. 2015), weathering resistance (Hon 1994) and mechanical properties such as hardness (Salca and Hiziroglu 2014). In this study, it is also used to describe resistance to handling and mechanical as well as natural wear.

The evaluation of the surface quality is rather complicated because of the inherent heterogeneity of wood. One approach for evaluation is the analysis of the surface roughness, which partly defines the perceived quality (Taylor et al. 1999), but also affects post-treatments such as painting and maintenance procedures. A rough surface is more susceptible to weathering damage because moisture and dirt easily accumulate in valleys, and protruding peaks and loose fibers are more prone to mechanical wear from use and, for example, wind-blown particles. This leads to uneven wear that affects the esthetics of the structure as

well as maintenance needs in the form of cleaning and recoating. Wood products are commonly machined to desired surface roughness, but this is more complicated with charred wood. It is obvious that the modification method heavily impacts the surface properties but quantifying the degree of impact is difficult. Ebner et al. (2021) used the term "char quality" to describe the consistency of the surface, which has a great impact on the durability in use. This included the thickness of the char layer, which has also been highlighted by Kymäläinen et al. (2020, 2022a, 2022b) and Kampe and Pfriem (2018). However, as reported by Kymäläinen et al. (2022b), the thickness does not necessarily explain the durability with respect to weathering, but the degree of wood degradation does, i.e., the flame-charred surfaces resist weathering better than the contact-charred ones because of more extensive compositional changes. This may be comparable to the term "quality" used for combustible chars, where the target is to eliminate impurities and maximize carbon content. Heavily degraded surfaces can be created with flame, especially when gas-fired. However, this type of surface is rough and friable, making it difficult to handle, clean and maintain. In contrast, a contact-charred surface is flat and hard which could provide an advantage in terms of handling, maintenance and service life performance. To further complicate comparisons, wood species have a major effect on the physical properties of char in that denser species produce a more compact char layer, which is less rough and has very promising weathering properties and performance (Kymäläinen et al. 2022b). As highlighted here, these treatments result in a complex charring response and more tools for analysis are needed than thickness or surface roughness alone. The objective of this study is to assess the use of surface roughness, abrasion and scratch resistance as quantifiable metrics to compare flame and contact charring treatments on soft and hardwood species to gain a more detailed understanding of the quality of the products. The macroscale measurements will be connected to nano- and microscale investigations on the carbon structures constituting the char that may also be used to describe the quality of the surface. A hard- and a softwood are compared to distinguish species-dependent responses to modifications and to investigate the potential of woods less used for exterior purposes.

Materials and methods

Preparation of specimens

Norway spruce (*Picea abies* (L.) Karst.) and silver birch (*Betula pendula* Roth.) were chosen as raw materials. Spruce is a softwood commonly used as cladding material, while birch is a hardwood not often used in exteriors, but one that presents an abundant raw material source throughout Europe. Flat-sawn sapwood boards were planed and cut to 100 mm × 100 mm (contact charring) and to 100 mm × 1000 mm (flame charring). Sample density was 450 and 620 kg/m^3 for spruce and birch, respectively. Material thickness was 24 and 25 mm, respectively. Samples were stored at 65% RH, 20 °C for at least 28 days prior to modification. The investigated samples were

contact charred at 320 °C for 30 min by exposing the pith side and using a weight of 16 kg on top to restrict sample distortion. The conditions were chosen based on previous experiments that aimed to create a crack-free surface with thick modified layer. Flame charring was implemented with a butane torch until consistent crack pattern (about 2 to 3 min). The modification methods have been reported in more detail also in Kymäläinen et al. (2022a, b, c). Prior to further experimenting the samples were stored at 65% RH, 20 °C. Unmodified spruce (referred to as SR in the text) and birch (BR) were used as references.

Elemental analysis

The elemental compositions of samples were analyzed with FlashSmart EA CHNS/O (Thermo Fischer Scientific, Waltham, MA, USA) on samples ground with a Wiley mill (Wiley Mini Mill 475-A, Thomas Scientific, Swedesboro, NJ, USA) to pass through a 20-mesh sieve. In the analysis, a 2–3 mg sample is first combusted, followed by flow through the catalyst and copper reduction phase with the carrier gas helium. The gases are carried through the GC column, which provides the separation of the combustion gases that are detected by a thermal conductive detector (TCD). The analyses were performed in triplicate.

Nanostructure of flame- and contact-charred surfaces

Differences in the char microstructure between the two modifications and two wood species were determined with a Cs-corrected high-resolution transmission electron microscope (HR-TEM) (JEM-2200FS, JEOL Ltd., Tokyo, Japan) with a 200 kV Schottky field emission gun (FEG) and an in-column Omega filter. For the analysis, contact- and flame-charred surfaces were extracted from both wood species. The char was scraped off with a razor blade and ground to fine powder. Images were recorded with a Gatan 4 k × 4 k UltraScan 4000 CCD camera and analyzed by Digital Micrograph (Gatan Inc., Pleasanton, CA, USA). Electron energy-loss spectroscopy (EELS) was included in the analysis. The spectra were collected using a selected-area aperture of about 1 µm, with a collection time of 10 s for the C edge.

Microstructure of surfaces illustrated by microscopy

The sample surfaces were imaged with scanning electron microscopy (SEM; Zeiss Sigma VP FE-SEM (Carl Zeiss Microscopy GmbH, Jena, Germany) with acceleration voltage of 3–5 kV. Prior to imaging, the samples were cut to about 1 mm × 1 mm × 1 mm pieces using a razor blade, oven-dried and sputter-coated with a 5-nm layer of platinum-palladium mix.

Surface roughness

3D profiles of the tested specimens' surfaces were captured by a VHX-500 microscope (Keyence, Itasca, USA). The measurement took place with the VH-Z100R

lens under standard conditions of 65% RH, 20 °C. Two parameters were determined during roughness testing: the arithmetical mean height of roughness (R_a) and average maximum height of profile (R_z). R_a is defined as the mean value of the distance of the point of the detected profile from the center line in the entire length of the measured section, and R_z is defined as the mean distance between the five lowest and the five highest points of the measured profile from the center line in the entire length of the measured section. For each specimen, four measurements of the same length were made in different parts of the surface. Results are the arithmetic mean of the measured values. The measured data were processed using Statistica 13 software (StatSoft Inc., Tulsa, OK, USA) and evaluated using one-factor analysis of variance (ANOVA) with Tukey's honest significant test (HSD test).

Abrasion resistance

The abrasion resistance of the unmodified and charred surfaces was analyzed with the Taber test (SFS EN ISO 7784–1:2016). A Model 503 standard abrasion tester (Teledyne Taber, North Tonawanda, NY, USA) was used with Calibrase CS-10 abrasive wheels with S33 sandpaper strips (Taber Industries, North Tonawanda, NY, USA). A load of 500 g was chosen, corresponding to normal use and cleaning operations as specified by the standard SFS EN ISO 7784–1:(2016). Prior to testing, three samples per each modification and species were cut to a thickness of 11 ± 1 mm with a band saw. A 9.5-mm hole was drilled in the middle for attachment. The samples were weighted at 0, 250 and 500 rotations and mass loss was determined, averaged between the three test specimens in a series. A Taber wear index was calculated as

$$\text{Lost mass (mg)} * 1000 \text{ rotations/actual number of rotations} \quad (1)$$

The samples were conditioned at 65% RH and 25 °C, different from the standard requirement of 50% RH. The char layer thickness was measured from cutouts using an Olympus SZX10 microscope (Olympus corp., Tokyo, Japan), and values were averaged between several measurements from transverse and radial surfaces.

Scratch test

The scratch test was performed using a pencil test according to SFS EN ISO 15184 (2020): Paints and varnishes–determination of film hardness by pencil test. Before starting the test, specimens were conditioned at 65% relative humidity (RH) and temperature of 20 °C until a constant mass was achieved. The pencil test was performed under standard conditions (65% RH, 20 °C) using a measuring device that pushes a pencil lead with a defined geometry over the paint surface at an angle of 45°. The hardness of the pencil lead was increased in steps until the testing surface was marked by visible defects. Pencils were divided according to hardness into groups 9B–B (soft, black), HB–hard black, F–firm and H–9H (hard). The result of the surface hardness was the highest hardness of the pencil lead at which no marking occurred.

Results and discussion

Nano-and microstructure of charred surfaces

Elemental analysis

The elemental analysis gives an overview of chemical changes in the samples in connection to modification (Table 1). Nitrogen and sulfur content was below detection limits, which is normal for biochars, especially those derived from wood (Antal and Grønli 2003). Carbon contents increase while hydrogen contents decrease. The change for C is close to linear, with $R^2 = 0.99$ (spruce) and 0.96 (birch), and $R^2 = 0.95$ (spruce) and 0.89 (birch) for H. The increase in C in comparison with reference samples is 18 and 56% (contact-charred birch BC, flame-charred birch BF) and 22 and 50% (contact-charred spruce SC, flame-charred spruce SF). Decreases in H are 8 and 41% (BC, BF) and 12 and 39% (SC, SF), indicating that spruce undergoes greater compositional change in contact charring, while the flame-charred surface is slightly further degraded in birch.

Wood pyrolysis is a well-known process with reactions taking place at general temperature regions. The elemental composition of char is dependent on the final temperature and holding time (Bourgois et al. 1989; Demirbas 2001; Antal and Grønli 2003). Complexity is brought about by differences in feedstock properties, such as wood species and type, density, moisture content and specimen size, as well as processing environments that may be inert, atmospheric, pressurized, etc. In given conditions, hardwoods usually pyrolyze faster and more completely than softwoods due to the differences in chemical composition, namely the larger amount and more labile structure of hemicelluloses (Nuopponen et al. 2005; Prins et al. 2006), and differences in lignin composition (Sudo et al. 1985; Anca-Couce and Obernberger 2016). The higher density affects the thermal conductance causing the birch to pyrolyze deeper than spruce wood. On the other hand, softwoods usually produce a higher yield of char because of a larger content of lignin (Demirbas 2001; Kambo and Dutta 2015; Anca-Couce and Obernberher 2016). The char line in a pyrolyzing piece of wood is set to about 280–350 °C, coinciding with the line where reactions change from endo- to exothermic (Browne 1958), although the rates of carbonization are very slow at this region (Antal and Grønli 2003). This is because heating wood between 250 and 400 °C causes a fast release of volatiles, a mix of organic compounds and noncondensable gases that usually escape without contributing to

Table 1 Relative contents (%) of carbon (C) and hydrogen (H) for reference spruce and birch (SR, BR), contact-charred spruce and birch (SC, BC) and flame-charred spruce and birch (SF, BF)

Modification	C (%)	H (%)	Modification	C (%)	H (%)
SR	47 (0.2)	5.9 (0.0)	BR	46 (0.1)	5.8 (0.0)
SC	57 (0.3)	5.2 (0.1	BC	54 (0.2)	5.4 (0.0)
SF	70 (0.2)	3.6 (0.1)	BF	72 (1.0)	3.4 (0.0)

Standard deviations between three measurements in parentheses

char formation (Antal and Grønli 2003). In contact charring, however, the long modification time, the large specimen size and the tight connection to the heated plate balance this out and at least a part of the volatiles is trapped for secondary reactions. The vapors are likely to escape more freely at the flame charring modification, but the higher thermal load causes more extensive structural degradation. Birch shows a slightly higher content of elemental carbon than spruce. This may be caused by larger evaporative loss of material from spruce, but the overall differences are very small.

Char nanostructure analyzed by transmission electron microscopy and electron energy-loss spectroscopy

The samples analyzed by HR-TEM did not reveal crystallites or significant layering of carbon, but an amorphous structure in both modifications and wood species (Fig. 1). The EELS spectra (Fig. 2), however, did reveal some graphitization with sp^2-hybridzation, most evident for the birch samples BC and BF. When comparing the different measurements, it was seen that the exact position and shape of the peaks varied with measuring location. This is typical for localized measurement techniques and can be seen, for example, in the shape of the spectrum of SF. According to Table 1, the sample is almost as extensively degraded

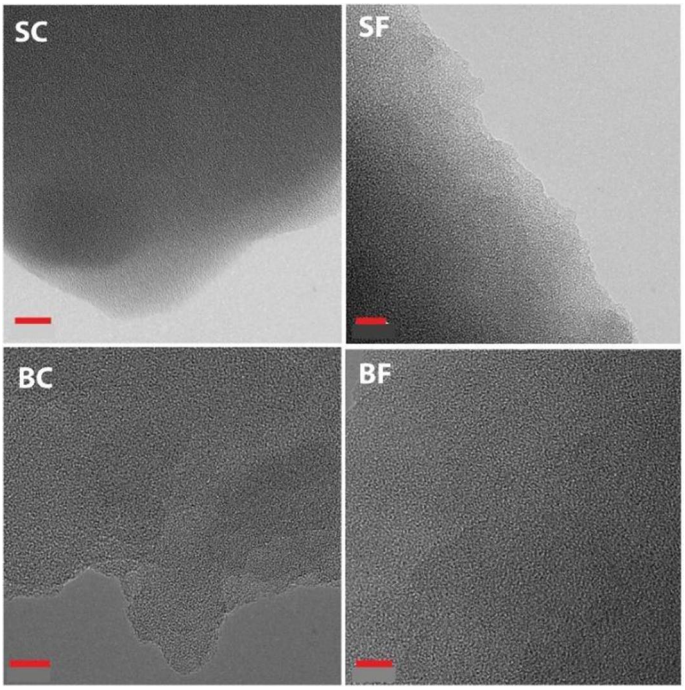

Fig. 1 HR-TEM images of contact-charred spruce (SC) (500x), flame-charred spruce (SF) (400x), contact-charred birch (BC) (500x) and flame-charred birch (BF) (500x) showing an amorphous, disordered carbon structure in all imaged samples. Bar = 10 nm

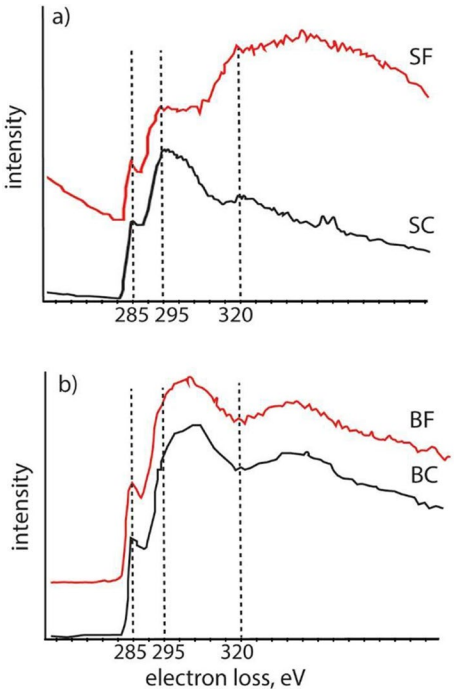

Fig. 2 Comparative presentation of core loss spectra (at 250–400 eV) of a) contact-charred (SC) and flame-charred (SF) spruce; b) contact-charred (BC) and flame-charred (BF) birch. The relevant peaks are marked at 285 eV revealing transitions from 1 s orbital to the π^* molecular orbital due to the presence of sp^2 bonding and at around 295 eV showing excitations to σ^* states. The area for multiple scattering resonances begins from around 320 eV

as BF, but the σ^* peak of SF is broad representing a more disordered structure, whereas the peak in BF is more intense, induced by transitions to σ^* orbitals. The π^* peaks are also more distinguishable in the birch samples, indicating a higher order of carbon. This may partly be a calibration issue, but it is indisputable that the extraction location of the sample affects the measurable composition. The char surface was removed for imaging by scraping with a razor blade from the very top surface, but it is possible that less charred areas from deeper beneath the surface may be included.

The char structure affects the quality of the carbonized surface in terms of durability in use, as a higher degree of order is hypothesized to increase the stability toward photochemical wear. The structure of biomass-derived carbon is dictated by the structure of the precursor material and the highest modification temperature (Yoo et al. 2018a, b). Translating the char quality into recalcitrance in use is a subject little studied, but some indication can be found from the structure of carbon black (CB) that is a much-used photostabilizer. Some CBs can act as superabsorbers of UV and visible light, as well as quench excited states of active species (Allen et al. 2000). CBs are usually produced from heavy fossil oil but can also be made from biomass (Toth et al. 2018). However, no grapelike (aciniform) fractal aggregates characteristic for CB (Long et al. 2013; Toth et al. 2018) were identified on our samples. Soot, on the other hand, is a similar substance to carbon black but exhibits more various nanostructures. Soot may be described as an impure form

of near-elemental carbon with a graphite-like structure that is formed in, for example, flaming combustion (Andreae and Gelencsér 2006) and is likely present in our samples.

In general, carbon–carbon bonds are strong and stable. The graphitic structures identified have a planar structure, where the bonds between atoms are very strong, but the bonds between planes are not. Therefore, graphite is sensitive to mechanical wear, but under atmospheric conditions, graphite also is an absolute inert material (Andreae and Gelencsér 2006). According to Lehmann and Joseph (2015), disordered porous materials transform into turbostatic carbon with randomly distributed graphitic stacking above 900 °C, while a more ordered structure forms above 1500 °C. The structure of the SF and BF is likely of this random kind, as the recorded surface temperatures were on average 800–1100 °C and no direct evidence of significant layering was seen. However, the graphitic nature of the flame-charred surface was also seen in Kymäläinen et al. (2022b) under Raman investigation, where practically no structural changes were seen in surfaces during one year of natural weathering.

The EELS profiles recorded from the high-loss area present both amorphous and graphitic features. The carbon K-edge in all the samples shows a clear π^* peak at 285 eV. At this point, the transition from 1 s to π^* orbital is closely related to the aromatic sp^2 ratio in carbon materials (Yoo et al. 2018b). Sharpening of the features that follow over the next 20 eV indicates increasing graphitization (Daniels et al. 2007). The birch peaks are more rounded, corresponding to a more amorphous structure. The π^* feature of graphite and amorphous carbon is visible in all modifications, but in spruce situated at a higher eV position than in birch. The SC EELS spectrum is practically identical to that obtained by Yoo et al. (2018b) for loblolly pine biochar prepared at 800 °C and the B spectra to that for biomass graphite with increased intensity of the multiple scattering resonance (MSR) structure starting from about 325 eV. This peak is generated by the local electron resonance in C–C bonding and can be used to calculate the bond lengths that on carbonaceous materials decrease with higher modification temperatures (Daniels et al. 2007). A shift to the right stands for increased aromatization. The broad shape of the SF spectrum differs from the rest, but other measurements, however, gave similar results to the BC, SC and BF, which further highlights the effect of the exact measuring location and the variability of the charred surface. The zero-loss region did not reveal notable differences between samples.

Surface details observed with scanning electron microscopy

Both wood species exhibit similar microstructures with microcracking of cell walls along the microfibril orientation and further cracking across the fiber in flame-charred samples (Fig. 3). The damage to cell walls is related to the sudden temperature increase that leads to fast expansion and evaporation of moisture and extractives that cause microcracking. Simultaneous shrinkage takes place due to uneven drying stresses and breakdown of interlayer bonds (Byrne and Nagel 1997; Pastor-Villegas et al. 1998). The contact-charred surfaces also shrunk noticeably, curving away from the heated surface. This cupping was stronger for spruce, but a more obvious

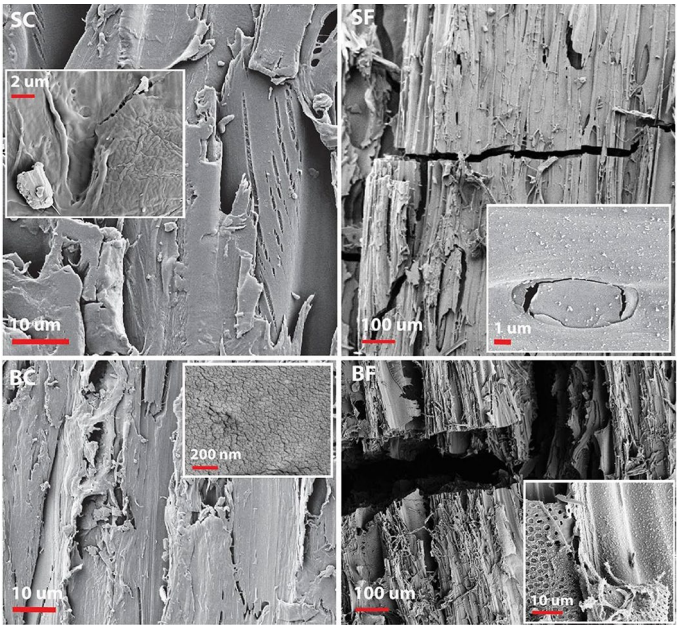

Fig. 3 Tangential (modified) surface of contact-charred spruce (SC) and birch (BC) and flame-charred spruce (SF) and birch (BF) with selected details in insets at 5 kV operating voltage. Samples SC and BC show a plasticized surface with cracking in longitudinal direction. Insets reveal microscale shrinkage (buckling) and cracking. Samples SF and BF show clean fracture lines also perpendicular to fiber, with insets exposing the granular deposits (partly evaporated extractive material) and an aspirated but fractured pit membrane on sample SF

shrinkage was observed on birch. The grainy structures found in both flame-charred species were absent from BC but were detected in parts of SC. This is likely extractive material that had begun to evaporate but became trapped between the surface and the hot plate and then cooled onto the surface after terminating the process. The absence of these granular deposits is in line with the elemental analysis, which suggests that SC is in fact further modified than BC, although the composition of extractives may also have an effect. For example, resin acids are only found in softwoods (Holmbom 1999). Similar grainy inner surfaces of cell lumens were detected on spruce contact-charred at 400 °C but were absent in similar samples charred at 250 °C (Kymäläinen et al. 2017).

A charred wood sample will largely retain the original macrostructure of the feedstock. Evaporation of moisture and extractives, as well as degradation products, will increase the porosity. The further the wood pyrolyzes, the more variable will be the pore structure and composition. An isotropic, structureless material marks a clear transition region between about 300 and 350 °C (Paris et al. 2005). At this point, the decomposition of hemicellulose and cellulose rapidly increases the fixed carbon content (Yoo et al. 2018a). As the crystalline structure of microfibrils is completely degraded, the wood has transformed into charcoal (Labbe et al. 2006). This is easily

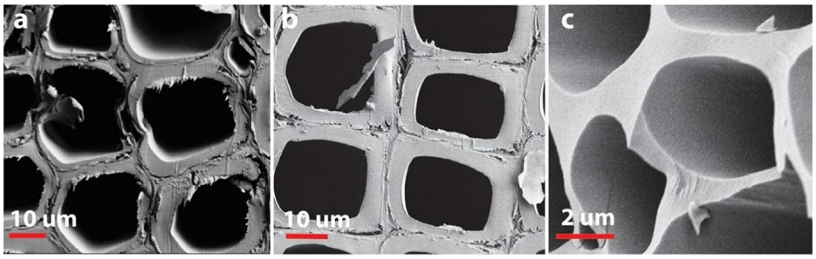

Fig. 4 Transverse sections of selected samples: a) unmodified spruce reference (SR), b) contact-charred spruce (SC), c) flame-charred birch (BF), showing the change from a layered cell wall to a bulky isotropic one

seen in Fig. 4, where cell wall layers are distinguishable in the reference sample of spruce (4a) and also in contact-charred spruce (4b). In Fig. 4c, BF, the layers have coalesced into a bulky material. The absence of a fibrous nature easily separates the charcoal from less modified contact-charred wood. For contact-charred wood, the cell wall modification has not reached a level where it would be clearly distinguishable from unmodified wood.

Surface quality in terms of roughness and resistance to wear

Surface roughness

The influence of charring method on the surface roughness is evident from the presented mean values R_a and R_z (Fig. 5). R_a is the arithmetic mean roughness of the profile and R_z the average value of the absolute values of the heights of five highest-profile peaks and the depths of five deepest alleys within the evaluation length. A statistically significant difference was observed between contact-charred and flame-charred specimens, as well as between flame-charred and reference specimens. A significant difference between contact-charred specimens and references was not confirmed. Specimens BC and SC achieved significantly lower values of surface roughness parameters (R_a and R_z) compared to BF and SF. The lowest surface roughness among the modified specimens was found for BC group with R_a of 14.36 µm. The SF group showed the highest surface roughness with R_a of 143 µm. The increased surface roughness is caused by the charring process: A heterogeneous modified layer with variable sized cracks is formed due to the uneven action of the flame on the surface during the process (Ebner et al. 2021), while a more homogeneous surface can be achieved by using the hot plate (Šeda et al. 2021; Kymäläinen et al. 2022c). However, it is necessary to use appropriate parameters of the modification process. Using our device, the surface began to crack at an approximate temperature of 330 °C practically regardless of modification duration. Surface damages caused by extensive cracking, that directly translate to increased roughness, have also been reported

by Kymäläinen et al. (2017) and Machová et al. (2021) using modification temperatures of 350 to 400 °C. The surface roughness of wood tends to decrease with commercial thermal modification (Unsal and Ayrilmis 2005; Bakar et al. 2013; Priadi and Hiziroglu 2013; Salca and Hiziroglu 2014), where temperatures stay below 300 °C.

The improved smoothness of contact-charred samples follows from plasticization of the surface and the weight used to restrict warping in the process. When exposed to heat, hemicelluloses and lignin pass their glass transition temperatures and become plastic. The strong evolution of gases (both condensable and noncondensable) also strongly affects the surface characteristics, although it is likely that most of these gases will evaporate from the transverse surfaces (the sides of the charring piece). A portion of these gases will nevertheless pass through the heated tangential surface and become trapped between the wood and the hot plate, as well as condensing on the sides of the sample upon cooling. The surface of contact-charred wood is basically in anoxic conditions due to tight contact with the heated plate. This is directly observable, as in suitable conditions, wood may autoignite at a surface temperature of about 250 °C (Babrauskas 2002). During our charring experiments, the plate was utilized at its limit of 500 °C for several minutes without combustion (glowing or flaming). These conditions cause the resin, extractives and other pyrolyzates to migrate toward the heated surface where they condense and harden as the wood piece is cooled down. Densification of wood surface by frictional heating produces the same kind of hard, glossy surface (Rautkari et al. 2010, 2012). The flame-charred surfaces were much rougher due to extensive cracking of the surface. The surface geometry is a result of macroscopic (corrugations, hollows, scratches, broken fibers), microscopic and submicroscopic imperfections (Kvietková et al. 2015). Birch char is more compact than spruce mostly due to higher material density and also more uniform due to lack of clear early-latewood boundaries (Biziks et al. 2019). The absence of resin canals also promotes formation of a smoother surface. In spruce, the boiling resin breaks the char surface and creates a different type of crack pattern.

Resistance to abrasion

The abrasion resistance of modified surfaces was much worse than that of references (Fig. 6). Heat treatment, in general, has an adverse effect on surface hardness due to deterioration of the cell wall structure (Salca and Hiziroglu 2014), and the abrasion resistance of thermally modified wood has therefore been reported to be lower compared to unmodified references (Aytin et al. 2015; Coelho et al. 2017), but also slightly higher in some cases (Welzbacher et al. 2009). The discrepancy is likely due to different wood species (black cherry, pine, beech), as the wear process is influenced by the anisotropy of wood (Karinkanta et al. 2011). On a wood sample with high wide annual rings, such as fast grown spruce, the earlywood sections wear out more than latewood sections. Birch on the other hand is a high strength material with moderate abrasion resistance in comparison with other common European woods (Klein et al. 2016). The values of flame-charred samples are lower (i.e.,

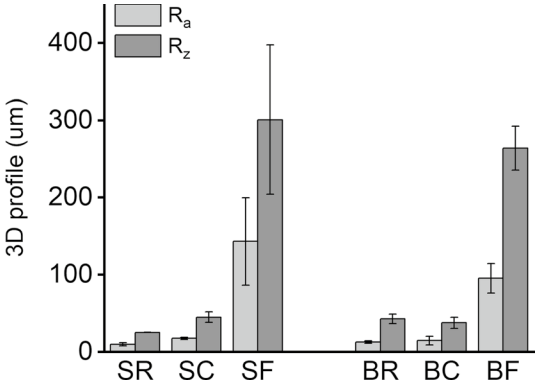

Fig. 5 Surface roughness of spruce reference (SR), contact-charred spruce (SC) and flame-charred spruce (SF) spruce, reference birch (BR), contact-charred birch (BC) and flame-charred birch (BF) depicted by arithmetic mean roughness R_a and ten-point height of irregularities R_z

showing higher abrasion resistance in comparison to contact-charred samples), but this is caused by the low density and thus low mass of the surface char. Under wood combustion conditions, both the porosity and initial char density are 10–20% lower compared to dry wood and decrease further if char undergoes secondary reactions (Ragland et al. 1991). Therefore, a gravimetric method is not very suitable for direct comparison between modifications. The mass loss between 250 and 500 rotations is also small on flame-charred samples because the surface was worn off already after 250 rotations, after which the recorded mass loss took place in the transition layer and the underlying unmodified wood. Figure 6 also shows that the transition layer is more intact in BF while on SF both the char and transition layers have been worn off. The discrepancy between the mass losses and the visual details must be due to differences in the char mass between the two species, or differences in the char plus transition layer thickness. The char plus transition zone thicknesses were about 1.1 mm (SF) to 4.5 mm (SC) and 1.1 mm (BF) to 4.8 mm (BC). Separating the char from transition zone is difficult using optical methods, as the transition is very gradual and visible mostly as coalescence of cell wall layers detected with high magnification as is presented in Fig. 4.

The Taber standard defines that samples must be as even and flat as possible. However, this was not possible with the SC samples, as cupping takes place during the modification. Using this modification, regime cupping is practically unavoidable as higher restrictive forces will compress the wood surface (Kymäläinen et al. 2017). A cupped sample will wear unevenly, possibly distorting the results: The wood surface was exposed more on the tangential-longitudinal sides than on the other two sides and the sample midpoint, which possibly explains the lower wear for SC in comparison with BC. In contrast, the birch samples were flat and even. Birch is less prone to cupping due to structural reasons. Shrinkage of birch is higher (Forest Products Laboratory 2010; Biziks et al. 2019) but due to more homogeneous wood material it is more uniform (Forest Products Laboratory 2010), resulting in less cupping distortion.

Scratch resistance

Compared to the large-scale abrasive test, the scratch test simulates surface durability more accurately, as the samples do not need to be perfectly level. The scratch resistance values determined using the pencil test are presented in Table 2. The pencil force was reduced against the standard from 7.35 N to 3.00 N ± 0.15 due to the low surface resistance of flame-charred specimens and in the effort to achieve better comparability between groups of measured specimens. Therefore, the measured values can be compared with the literature only at the level of the surface resistance difference between the modified samples and the references. As assumed, the flame-charred specimens BF and SF achieved the lowest resistance values due to extensive structural degradation of the surface and reduced strength. The highest resistance among the modified specimens was achieved by the BC group, which is in line with the initial observation of denser woods forming denser chars. The results show a significantly lower resistance of SR and SC groups compared to BR and BC. This significant difference confirms the fundamental influence of the anatomical structure of individual wood species on their surface properties. The charred surfaces did not differ from each other.

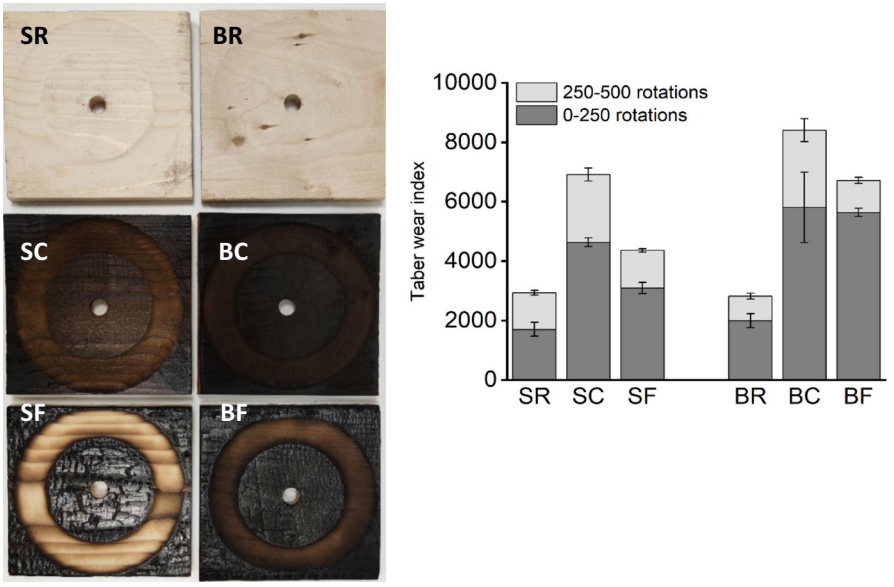

Fig. 6 Abraded samples after 500 rotations (left); Taber wear index for spruce reference (SR), contact-charred spruce (SC) and flame-charred spruce (SF) spruce, reference birch (BR), contact-charred birch (BC) and flame-charred birch (BF) after 250 and 500 rotations (right)

Table 2 Measured data of scratch resistance using pencil test

Modification	Pencil hardness	Modification	Pencil hardness
SR	8B	BR	2B
SC	< 9B	BC	5B
SF	< 9B	BF	< 9B

Conclusion

Contact and flame charring methods were compared in terms of surface characteristics of Norway spruce and silver birch. Although surface roughness is a common method to evaluate the quality of a wood product, the complexity of the carbonization reactions in connection with modification method and wood species requires more in-depth investigation of the characteristics. The carbon content increases with treatment severity as expected. Elemental analysis revealed the differences between modifications and SEM imaging can be used to detect the transition from wood to char, at least for flame-charred surfaces. The carbon structures were further analyzed with TEM and EELS, and indication of graphitization and thus higher order of carbon structures were seen both in contact- and flame-charred surfaces. A more ordered structure is hypothesized to be more resistant toward stresses such as weathering. This has already been directly observed for similarly modified wood surfaces during natural weathering experiments. A flame-charred surface is suggested to be composed of amorphous carbon with random graphitic stacking, a structure commonly seen in biochars. Thus, the qualities used to describe these biochars, such as content of elemental carbon and processing temperature, can also be used to describe carbonized surfaces. The lower modification temperature of contact-charred specimens suggests dominant amorphous characteristics, but the modification process promotes formation of other favorable properties, such as a higher surface smoothness and homogeneity. It was seen that charred birch surfaces have a higher quality than spruce surfaces due to a denser, more homogeneous structure that responds well to carbonization. The nanostructure of birch showed higher carbon ordering with graphitization, although it is emphasized that the exact composition is highly dependent on measurement location. Contact-charred birch surfaces did not differ from spruce in terms of roughness, but the BF samples were more even and smooth compared to SF. Overall, the contact charring result is less dependent on species. The birch surfaces were also found more compact in scratch tests and exhibited a transition layer more resistant to abrasion. The surface roughness test appears to correlate with the perceived quality of contact-charred woods as has also been shown for unmodified woods. For charred surfaces, the scratch resistance test is a better method to assess surface quality in comparison to abrasion. The gravimetric measurement of material lost in abrasion is not comparable due to extensive changes in mass and density. Further, the dimensional distortion of contact-charred (soft)wood is a major error source. The results show that comparing woods modified with different surface carbonization techniques is challenging, but within a

modification regime, different wood species/types can be adequately compared with several methods.

Acknowledgements Support from the Academy of Finland granted for project CHARFACE (project number 13315408) is highly appreciated by lead author. The authors acknowledge the help of research laboratory assistant Mikael Hytti. J.D. and V. Š. are grateful for the European Union's Horizon 2020 research and innovation programme under Grant Agreement No. 952314. We also acknowledge the OtaNano Nanomicroscopy Center (NMC) for provision of equipment and sincerely thank Senior scientist Jiang Hua for his expertise in transmission electron microscopy and EELS.

Author contributions M.K., M.S. and J.D. designed the experimental setup; M.K., M.S., J.D. and V.S. carried out the experiments and processed the data; M.K. prepared the figures and wrote the main manuscript text; L.R. acted as supervisor; All authors reviewed the manuscript.

Funding Open Access funding provided by Aalto University.

Declarations

Conflict of interest The authors declare no competing interests.

References

Allen NS, Pena JM, Edge M, Liauw CM (2000) Behaviour of carbon pigments as excited state quenchers in LDPE. Polym Deg Stabil 67(3):563–566

Anca-Couce A, Obernberger I (2016) Application of a detailed biomass pyrolysis kinetic scheme to hardwood and softwood torrefaction. Fuel 167:158–167. https://doi.org/10.1016/j.fuel.2015.11.062

Andreae MO, Gelencsér A (2006) Black carbon or brown carbon? The nature of light-absorbing carbonaceous aerosols. Atmos Chem Phys Discuss 6:3419–3463

Antal MJ, Grønli M (2003) The art, science, and technology of charcoal production. Ind Eng Chem Res 42:1619–1640

Aytin A, Korkut S, As N, Ünsal Ö, Günduz G (2015) Effect of heat treatment of wild cherry wood on abrasion resistance and withdrawal capacity of screws. Drvna Ind 66(4):297–303

Babrauskas V (2002) Ignition of wood: a review of the state of the art. J Fire Prot Eng 12:163–189. https://doi.org/10.1106/104239102028711

Bakar BFA, Hiziroglu S, Tahir PM (2013) Properties of some thermally modified wood species. Mater Design 43:348–355. https://doi.org/10.1016/j.matdes.2012.06.054

Biziks V, Van Acker J, Militz H, Grinins J, van den Bulcke J (2019) Density and density profile changes in birch and spruce caused by thermo-hydro treatment measured by X-ray computed tomography. Wood Sci Technol 53:491–504. https://doi.org/10.1007/s00226-018-1070-6

Bourgois J, Bartholin MC, Guyonnet R (1989) Thermal treatment of wood: analysis of the obtained product. Wood Sci Technol 23:303–310

Browne FL (1958) Theories of the combustion of wood and its control. A survey of the literature. U.S. Forest Service Research Paper FPL 2136. Madison, Wisconsin

Byrne CE, Nagle DC (1997) Carbonization of wood for advanced materials application. Carbon 35(2):259–266

Čermák P, Dejmal A, Paschová Z, Kymäläinen M, Dömény J, Brabec M et al (2019) One-sided surface charring of beech wood. J Mater Sci 54:9497–9506. https://doi.org/10.1007/s10853-019-03589-3
Coelho MU, del Menezzi C, de Souza MR (2017) Abrasion resistance of Pinus wood subjected to thermomechanical treatments. Pro Ligno 13(4):94–100
Daniels H, Brydson R, Rand B, Brown A (2007) Investigating carbonization and graphitization using electron energy loss spectroscopy (EELS) in the transmission electron microscope (TEM). Philos Mag 87(27):4073–4092. https://doi.org/10.1080/14786430701394041
Demirbaş A (2001) Biomass to charcoal, liquid, and gaseous products via carbonization process. Energ Source 23:579–587
Ebner DH, Barbu M-C, Čermák P (2021) Surface modification of spruce and fir sawn-timber by charring on the traditional Japanese method–yakisugi. Polymers 13:1662. https://doi.org/10.3390/polym13101662
Ebner DH, Barbu M-C, Gryc V, Čermák P (2022) Surface charring of Silver fir wood cladding using an enhanced traditional Japanese yakisugi method. BioResources 17(2):2031–2042
Forest Products Laboratory (2010) Wood handbook—Wood as an engineering material. General Technical Report FPL-GTR-190. Madison, WI: U.S. Department of Agriculture, Forest Service, Forest Products Laboratory. p 508
Hiziroglu S, Zhong ZW, Tan HL (2013) Measurement of bonding strength of pine, kapur and meranti wood species as function of their surface quality. Measurement 46(9):3198–3201. https://doi.org/10.1016/j.measurement.2013.05.005
Holmbom B (1999) Extractives. In: Sjöström E, Alén R (eds) Analytical methods in wood chemistry, pulping, and papermaking. Springer Series in Wood Science. Springer, Berlin, Heidelberg. https://doi.org/10.1007/978-3-662-03898-7_5
Hon DNS (1994) Degradative effects of ultraviolet light and acid rain on wood surface quality. Wood Fiber Sci 26(2):185–191
Kambo HS, Dutta A (2015) A comparative review of biochar and hydrochar in terms of production, physico-chemical properties and applications. Renew Sust Energ Rev 45:359–378. https://doi.org/10.1016/j.rser.2015.01.050
Kampe A, Pfriem A (2018) A note on artificial weathering of spruce (*Picea abies*) with a carbonised layer. Int Wood Prod J 9(2):86–89
Karinkanta P, Illikainen M, Niinimäki J (2011) The effect of anisotropicity of Norway spruce (*Picea abies*) during two-body abrasion. Wear 272(1):38–42. https://doi.org/10.1016/j.wear.2011.07.004
Klein A, Bockhorn O, Mayer K, Grabner M (2016) Central European wood species: characterization using old knowledge. J Wood Sci 612:194–202. https://doi.org/10.1007/s10086-015-1534-3
Kvietková M, Gaff M, Gašparík M, Kaplan L, Barcík Š (2015) Surface quality of milled birch wood after thermal treatment at various temperatures. BioResources 10(4):6512–6521
Kymäläinen M, Hautamäki S, Lillqvist K, Segerholm K, Rautkari L (2017) Surface modification of solid wood by charring. J Mater Sci 52:6111–6119. https://doi.org/10.1007/s10853-017-0850-y
Kymäläinen M, Turunen H, Čermák P, Hautamäki S, Rautkari L (2018) Sorption-related characteristics of surface charred spruce wood. Materials 11:2083. https://doi.org/10.3390/ma11112083
Kymäläinen M, Turunen H, Rautkari L (2020) Effect of weathering on surface functional groups of charred Norway spruce cladding panels. Forests 11:1373–1382
Kymäläinen M, Sjökvist T, Dömény J, Rautkari L (2022a) Artificial weathering of contact-charred wood–the effect of modification duration, wood species and material density. Materials 15:3952. https://doi.org/10.3390/ma15113951
Kymäläinen M, Lourençon TV, Lillqvist K (2022b) Natural weathering of soft- and hardwoods modified by contact and flame charring methods. Eur J Wood Prod 80:1309–1320. https://doi.org/10.1007/s00107-022-01864-w
Kymäläinen M, Dömény J, Rautkari L (2022c) Moisture sorption of wood surfaces modified by one-sided carbonization as an alternative to traditional façade coatings. Coatings 12(9):1273. https://doi.org/10.3390/coatings12091273
Labbé N, Harper D, Rials T, Elder T (2006) Chemical structure of wood charcoal by infrared spectroscopy and multivariate analysis. J Agric Food Chem 54:3492–3497. https://doi.org/10.1021/jf053062n
Lehmann J, Joseph S (2015) Biochar for Environmental Management: Science, Technology and Implementation, 2nd. ed. Routledge, Taylor and Francis Group: New York, London

Long CM, Nascarella MA, Valberg PA (2013) Carbon black vs. black carbon and other airborne materials containing elemental carbon: Physical and chemical distinctions. Environ Pollut 181:271–286. https://doi.org/10.1016/j.envpol.2013.06.009

Machová D, Oberle A, Zárybnická L, Dohnal J, Šeda V, Dömény J et al (2021) Surface characteristics of one-sided charred beech wood. Polymers 13:1551–1566. https://doi.org/10.3390/polym13101551

Nuopponen M, Vuorinen T, Jämsä S, Viitaniemi P (2005) Thermal modification in softwood studied by FT-IR and UV Resonance Raman spectroscopies. J Wood Chem Technol 24(1):13–26. https://doi.org/10.1081/WCT-120035941

Paris O, Zollfrank C, Zickler GA (2005) Decomposition and carbonisation of wood biopolymers–a microstructural study of softwood pyrolysis. Carbon 43:53–66. https://doi.org/10.1016/j.carbon.2004.08.034

Pastor-Villegas J, Durán-Valle CJ, Valenzuela-Calahorro C, Gómez-Serrano V (1998) Organic chemical structure and structural shrinkage of chars prepared from rockrose. Carbon 26(9):1251–1256

Priadi T, Hiziroglu S (2013) Characterization of heat treated wood species. Mater Design 49:575–582. https://doi.org/10.1016/j.matdes.2012.12.067

Prins MJ, Ptasinski KJ, Janssen FJJG (2006) Torrefaction of wood Part 1. Weight loss kinetics. J Anal Appl Pyrolysis 77:28–34. https://doi.org/10.1016/j.jaap.2006.01.00

Ragland KW, Aerts DJ, Baker AJ (1991) Properties of wood for combustion analysis. Bioresource Technol 37:161–168

Rautkari L, Hänninen T, Johansson L-S, Hughes M (2012) A study by X-ray photoelectron spectroscopy (XPS) of the chemistry of the surface of Scots pine (Pinus sylvestris L.) modified by friction. Holzforschung 66(1):93–96

Rautkari L, Kutnar A, Hughes M, Kamke FA (2010) Wood surface densification using different methods. In: Proceedings, 11th world conference on timber engineering (WCTE), pp 20–24 June, 2010, Trentino, Italy

Salca E-A, Hiziroglu S (2014) Evaluation of hardness and surface quality of different wood species as function of heat treatment. Mater Design 62:416–423. https://doi.org/10.1016/j.matdes.2014.05.029

Šeda V, Machová D, Dohnal J, Dömény J, Zárybnická L, Oberle A et al (2021) Effect of one-sided surface charring of beech wood on density profile and surface wettability. Appl Sci 11:4086

SFS-EN ISO 15184 (2020) Paints and varnishes–Determination of film hardness by pencil test. Finnish Standards Association, Helsinki

SFS-EN ISO 7784–1 (2016) Paints and varnishes–Determination of resistance to abrasion–Part 1: Method with abrasive-paper covered wheels and rotating test specimen. Finnish Standards Association, Helsinki

Sudo K, Shimizu K, Sakurai K (1985) Characterization of steamed wood lignin from beech wood. Holzforschung 39(5):281–288. https://doi.org/10.1515/hfsg.1985.39.5.281

Taylor JB, Carrano AL, Lemaster RL (1999) Quantification of process parameters in a wood sanding operation. Forest Prod J 49(5):41–46

Toth P, Vikström T, Molinder R, Wiinikka H (2018) Structure of carbon black continuously produced from biomass pyrolysis oil. Green Chem 20:3981–3992. https://doi.org/10.1039/C8GC01539B

Unsal O, Ayrilmis N (2005) Variations in compression strength and surface roughness of heat-treated Turkish river red gum (*Eucalyptus camaldulensis*) wood. J Wood Sci 51:405–409

Welzbacher C, Brischke C, Rapp A, Koch S, Hofer S (2009) Performance of thermally modified timber (TMT) in outdoor application–durability, abrasion, and optical appearance. Drvna Ind 60(2):75–82

Yoo S, Kelley S, Tilotta DC, Park S (2018a) Structural characterization of Loblolly pine derived biochar by X-ray diffraction and electron energy loss spectroscopy. ACS Sust Chem Eng 6:2621–2629. https://doi.org/10.1021/acssuschemeng.7b04119

Yoo S, Chun C-C, Kelley SS, Park S (2018b) Graphitization behavior of loblolly pine wood investigated by in situ high temperature X-ray diffraction. ACS Sust Chem Eng 6:9113–9119. https://doi.org/10.1021/acssuschemeng.8b01446

Authors and Affiliations

Maija Kymäläinen[1] · Jakub Dömény[2] · Matthew Schwarzkopf[3] · Vit Šeda[2] · Lauri Rautkari[1]

✉ Maija Kymäläinen
maija.kymalainen@gmail.com

[1] Department of Bioproducts and Biosystems, School of Chemical Technology, Aalto University, P.O. Box 16300, 00076 Aalto, Finland

[2] Department of Wood Science and Technology, Faculty of Forestry and Wood Technology, Mendel University in Brno, Zemědělská 3, 613 00 Brno, Czech Republic

[3] Innorenew CoE, Livade 6A, 6310 Izola, Slovenia